Developmental Cell
Article

Spatial Coordination between Stem Cell Activity and Cell Differentiation in the Root Meristem

Laila Moubayidin,[1] Riccardo Di Mambro,[1] Rosangela Sozzani,[2,3] Elena Pacifici,[1] Elena Salvi,[1] Inez Terpstra,[4] Dongping Bao,[4] Anja van Dijken,[4] Raffaele Dello Ioio,[1,7] Serena Perilli,[1] Karin Ljung,[5] Philip N. Benfey,[2] Renze Heidstra,[4,8] Paolo Costantino,[1] and Sabrina Sabatini[1,6,*]

[1]Dipartimento di Biologia e Biotecnologie, Laboratory of Functional Genomics and Proteomics of Model Systems, Università di Roma, Sapienza, via dei Sardi, 70-00185 Rome, Italy
[2]Department of Biology and Duke Center for Systems Biology, Duke University, Durham, NC 27708, USA
[3]Dipartimento di Biologia e Biotecnologie, Universita di Pavia, via Ferrata, 9-27100 Pavia, Italy
[4]Faculty of Science, Department of Biology, Section of Molecular Genetics, Utrecht University, 3512 JE Utrecht, The Netherlands
[5]Department of Forest Genetics and Plant Physiology, Umeå Plant Science Centre, Swedish University of Agricultural Sciences, SE-901 83 Umeå, Sweden
[6]Istituto Pasteur-Fondazione Cenci Bolognetti, 00185 Rome, Italia
[7]Present address: Max Planck Institute for Plant Breeding Research, 50829 Cologne, Germany
[8]Present address: Plant Developmental Biology, Department of Plant Science, Wageningen University, 6708 LX Wageningen, The Netherlands
*Correspondence: sabrina.sabatini@uniroma1.it
http://dx.doi.org/10.1016/j.devcel.2013.06.025

SUMMARY

A critical issue in development is the coordination of the activity of stem cell niches with differentiation of their progeny to ensure coherent organ growth. In the plant root, these processes take place at opposite ends of the meristem and must be coordinated with each other at a distance. Here, we show that in *Arabidopsis*, the gene *SCR* presides over this spatial coordination. In the organizing center of the root stem cell niche, SCR directly represses the expression of the cytokinin-response transcription factor ARR1, which promotes cell differentiation, controlling auxin production via the *ASB1* gene and sustaining stem cell activity. This allows SCR to regulate, via auxin, the level of *ARR1* expression in the transition zone where the stem cell progeny leaves the meristem, thus controlling the rate of differentiation. In this way, SCR simultaneously controls stem cell division and differentiation, ensuring coherent root growth.

INTRODUCTION

In multicellular organisms, stem cell division and differentiation of the progeny cells must be coordinated to ensure coherent growth. In the *Arabidopsis* root, stem cells reside in the apical region of the meristem, where they surround a small group of organizer cells. Together, they form a stem cell niche (SCN) (van den Berg et al., 1997; Scheres, 2007) (Figure 1A). As in the animal stem cell niche, the organizer cells, called the quiescent center (QC), maintain the divisional activity of the surrounding stem cells by means of unknown short-range signals (van den Berg et al., 1997; Scheres, 2007). Stem cells generate transit-amplifying cells, which undergo additional divisions and then differentiate in the transition zone (TZ; Figure 1A) (Moubayidin et al., 2009; Perilli et al., 2010). For meristem maintenance, and therefore continuous root growth, the rate of differentiation of transit-amplifying cells must be equal to the rate of generation of new cells. We have shown that, in the TZ, this balance is ensured by the interaction between two hormones: cytokinin, which promotes cell differentiation (Dello Ioio et al., 2007), and auxin, which promotes cell division (Blilou et al., 2005). In particular, cytokinins are perceived at the TZ by the *ARABIDOPSIS* HISTIDINE KINASE 3 (AHK3) cytokinin receptor, which transfers the signal, via a phosphorelay, into the nucleus and activates two cytokinin primary response transcription factors, *ARABIDOPSIS* RESPONSE REGULATOR 1 (ARR1) and *ARABIDOPSIS* RESPONSE REGULATOR 12 (ARR12) (Hwang et al., 2012). These genes activate the transcription of the *SHORT HYPOCOTYL 2* gene (*SHY2*), an inhibitor of auxin signaling (Tian et al., 2002; Dello Ioio et al., 2008). SHY2, in turn, negatively regulates the expression of several *PIN-FORMED* (*PIN*) genes encoding auxin transport facilitators (Friml, 2010), thus limiting auxin transport and distribution and allowing cell differentiation (Dello Ioio et al., 2008; Moubayidin et al., 2010).

Root SCN maintenance requires the activity of SCR, a member of the GRAS family of transcription factors (Di Laurenzio et al., 1996; Pysh et al., 1999; Lee et al., 2008; Sabatini et al., 2003). SCR was originally identified as a key factor regulating the asymmetric cell division producing the cortex and endodermis (Di Laurenzio et al., 1996; Heidstra et al., 2004; Cui et al., 2007). More recently, it has also been shown to be involved in the specification of xylem cell types within the vascular tissue (Carlsbecker et al., 2010) and in controlling ground tissue stem cell asymmetric division (Sozzani et al., 2010; Cruz- Ramírez et al., 2012). In addition, SCR has been shown to be necessary and sufficient, when acting in the QC cells, to sustain QC functions and, as a consequence, the surrounding stem cells (Sabatini et al., 2003), but the molecular mechanism for this activity remains unknown.

While molecular mechanisms regulating stem cell division (Spradling et al., 2001; Scheres, 2007; Sablowski, 2011; Wolpert

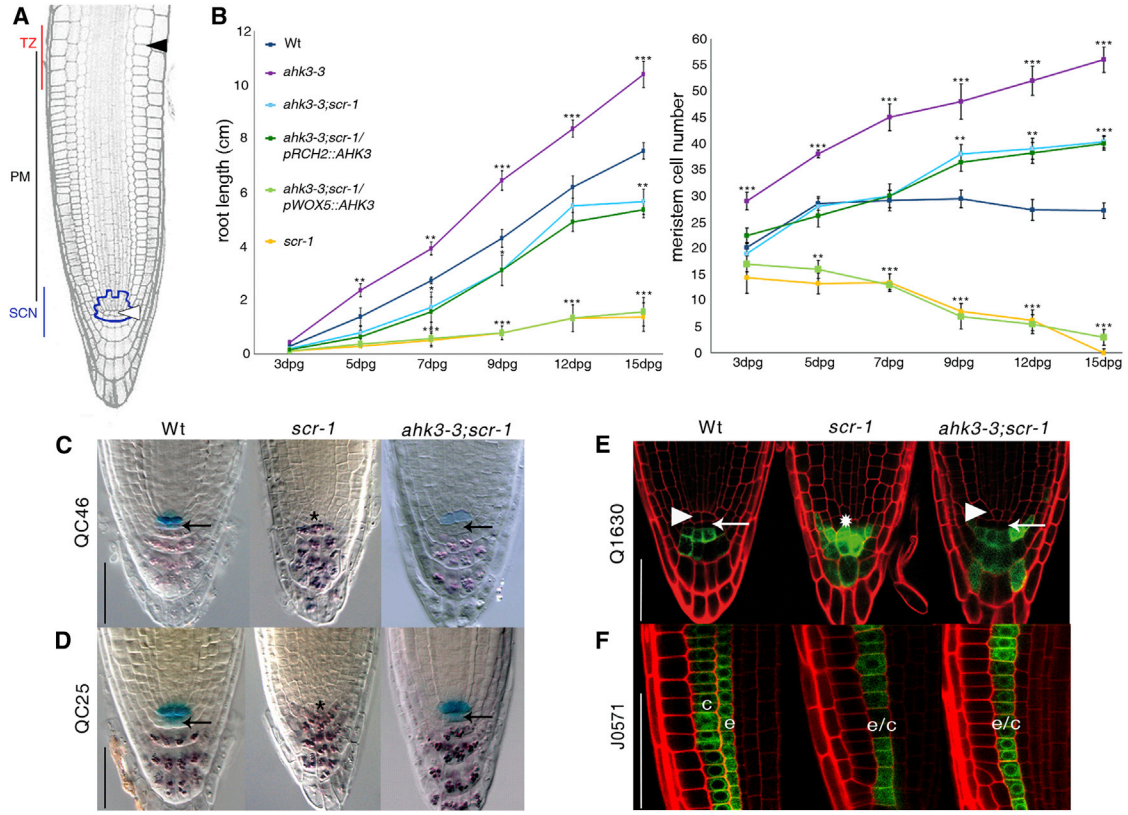

Figure 1. SCR Maintains SCN Activity by Suppressing AHK3-Mediated Differentiation Input in the QC Cells

(A) Longitudinal section of the *Arabidopsis* root meristem. SCN, stem cell niche (highlighted in blue); PM, proximal meristem; TZ, transition zone. The white and black arrowheads include meristematic cortex file, indicating QC and the last meristematic cortical cell, respectively.

(B) From left to right, root length and meristem cell number measured over time of wild-type (WT), *scr-1*, *ahk3-3*, *ahk3-3;scr-1*, *ahk3-3;scr-1/pRCH2::AHK3*, and *ahk3-3;scr-1/pWOX5::AHK3*. Dpg, days postgermination. Error bars represent SD; *p < 0.05, **p < 0.01, ***p < 0.001 (Student's t test).

(C–E) Elimination of AHK3 activity rescues SCN defect of *scr-1* mutant. Expression of *QC46* and *QC25* (C and D) and *Q1630* markers (E) in WT, *scr-1*, and *ahk3-3;scr-1* root tips. (C and D) Double labeling of QC and differentiated columella cells visualized by QC-specific markers and amyloplast staining, respectively. Note that the black arrows indicate restoration of columella stem cells activity in the *ank3-3;scr-1* double mutant (C). Lack of *Q1630* expression in the columella stem cells (white arrows) indicates that columella stem cell activity is restored in the *ahk3-3;scr-1* double mutant. White arrowheads indicate QC position in WT and *ahk3-3;scr-1*. Asterisk indicates the presumptive position of QC cells in the *scr-1* mutant.

(F) SCR-mediated cytokinin signaling suppression is not necessary for endodermis activity. *J0571* expression in WT, *scr-1*, and *ahk3-3;scr-1*. Note the lack of asymmetric cell division necessary to generate properly cortex (c) and endodermis (e) tissues in *scr-1* (Di Laurenzio et al., 1996) and in the *ahk3-3;scr-1* double mutant. The resulting monolayer is indicated by c/e. Scale bar represents 50 μm in all panels.

See also Figure S1.

and Tickle, 2011) and transit-amplifying cell differentiation (Wolpert and Tickle, 2011; Dello Ioio et al., 2008; Tsukagoshi et al., 2010) have been described, little is known about how these two events are coordinated (Mondal et al., 2011).

Here, we show that SCR acts in the QC to control, at the same time, stem cell activity and the differentiation of their progeny by cell-autonomously preventing expression of the cytokinin response regulator *ARR1* in the QC, and non-cell-autonomously controlling *ARR1* expression in the TZ via auxin.

RESULTS

SCR Sustains Stem Cell and Meristem Activity by Suppressing Cytokinin Perception

We hypothesized that the coordination between stem cell activity in the SCN and cell differentiation in the TZ might be effected by a genetic interaction between key molecular components directly regulating each zone of the root meristem. We therefore asked whether a genetic interaction may exist between SCR, which is involved in QC and stem cell maintenance (Sabatini et al., 2003), and the cytokinin receptor AHK3, which mediates cell differentiation in the TZ (Dello Ioio et al., 2007). Mutation in the *SCR* gene results in meristem consumption and arrested root growth a few days after germination (Figure 1B), due to defective QC and stem cell activities (Figures 1C–1E) (Sabatini et al., 2003). Mutation in the *AHK3* gene results in an enlarged meristem and a longer root, due to delayed cell differentiation in the TZ (Figure 1B) (Dello Ioio et al., 2007). Interestingly, in *ahk3-3;scr-1* double mutants, meristem size and root growth are maintained over time (Figures 1B, S1A, and S1D available online). In the *scr-1* mutant, the QC markers *QC25* and *QC46* are absent due to loss of QC identity, while cells immediately

below the QC, at the position of columella stem cells, acquire differentiation markers such as amyloplasts and the *Q1630* marker (Figures 1C–1E) (Sabatini et al., 2003). By contrast, in the *ahk3-3;scr-1* double mutant, *QC25* and *QC46* expression is restored and no amyloplasts or *Q1630* expression is detected within the columella stem cell layer (Figures 1C–1E). In addition, root hairs and xylem strands, characteristic of fully differentiated epidermal and vascular cells, are present in *scr-1* meristems (Figure S1D) (Sabatini et al., 2003) but are absent from the *ahk3-3;scr-1* root meristem (Figure S1D). These data indicate that in *ahk3-3;scr-1* roots, stem cell maintenance is restored, leading to meristem maintenance and root growth. Thus, this suggests that SCR sustains stem cell and meristem activity by suppressing cytokinin perception. It is important to note that the *ahk3-3;scr-1* double mutant still displays an undivided ground tissue layer (Figure 1F) (Di Laurenzio et al., 1996) and a lack of protoxylem cells characteristic of the *scr-1* mutant (Figure S1B) (Carlsbecker et al., 2010), suggesting that its role in stem cell regulation is independent of its developmental role in these tissues.

SCR Suppresses Cytokinin Activity in the QC

Comparison of the expression patterns of *SCR* (Wysocka-Diller et al., 2000) and *AHK3* (Dello Ioio et al., 2007) (Figure S1C) suggested that these genes might genetically interact either in the QC, where SCR maintains QC identity (Sabatini et al., 2003), or in the endodermis of the TZ, where AHK3 mediates cell differentiation (Dello Ioio et al., 2007). To determine if and where the interaction occurs, we exploited a tissue-specific complementation approach to restore AHK3 activity (and thus cytokinin perception) either specifically in the QC or in the TZ of the *ahk3-3;scr-1* double mutant. To accomplish this, we drove *AHK3* expression with the *WUS-RELATED HOMEOBOX 5* (*WOX5)* promoter, which confers expression in the QC (Sarkar et al., 2007), and the *ROOT CLAVATA HOMOLOG 2* (*RCH2*) promoter, which confers expression in the TZ (Dello Ioio et al., 2007) (Figure S1C). In *ahk3-3;scr-1/pRCH2::AHK3* plants, both meristem size and root growth are indistinguishable from that of *ahk3-3*;*scr-1* (Figures 1B, S1A, and S1D). By contrast, the meristem of *ahk3-3*;*scr-1/pWOX5::AHK3* plants is consumed and root growth arrested as in the *scr-1* mutant (Figures 1B, S1A, and S1D). These results indicate that AHK3 and SCR interact in the QC, thus suggesting that SCR maintains the SCN and meristem activity by suppressing cytokinin signaling in these cells.

SCR Prevents SCN Differentiation and Maintains Meristem Activity by Suppressing *ARR1*

To understand how SCR represses cytokinin-mediated cell differentiation, we examined *AHK3* expression in the *scr-1* mutant by means of quantitative RT-PCR (qRT-PCR) analysis and a *pAHK3::AHK3:GUS* translational fusion (Dello Ioio et al., 2007). Interestingly, neither the expression nor the accumulation of AHK3 (Figures S2A and S2B) is altered in the *scr-1* mutant. We have previously shown that AHK3 controls the rate of cell differentiation in the TZ via the activation of two primary cytokinin response transcription factors: ARR1 and ARR12 (Dello Ioio et al., 2007; Moubayidin et al., 2010). We therefore analyzed the expression of *ARR1* and *ARR12* in *scr-1* utilizing *pARR1::ARR1:GUS* and *pARR12::ARR12:GUS* translational fusions (Dello Ioio et al., 2007; Moubayidin et al., 2010) as well as by qRT-PCR. Neither ARR12 protein (Figure S2A) nor messenger RNA (mRNA) (Figure S2B) levels are altered, while the levels of both mRNA and protein of *ARR1* are upregulated in both *scr-1* and *scr-4* mutant backgrounds (Figures 2A and 2B, *scr-1*, and Figures 3A and 3B, *scr-4*). The ARR1 protein, which is normally expressed in all tissues of the TZ, was ectopically expressed in the proximal meristem, including the SCN, of *scr* plants (Figures 2B, 3A, and 3B). This suggests that SCR maintains the activities of both QC and stem cells by suppressing *ARR1* transcription, and therefore cytokinin signaling, in the QC. To further test this hypothesis, we analyzed the root phenotype of plants carrying a double mutation in both *SCR* and *ARR1* genes. Similar to the *ahk3-3*;*scr-1* double mutant, the *arr1-4*;*scr-1* double mutant displays sustained meristem and indeterminate root growth (Figures 2C, S2C, and S2D) due to an active SCN, as visualized by the presence of QC markers absent in the *scr-1* mutant (Figures 2D and S2E). In addition, amyloplasts were absent from the columella stem cells (Figures 2D and Figure S2E). By contrast, the root phenotype of the *arr12-1;scr-1* double mutant was indistinguishable from that of *scr-1* (Figures 2C, S2C, and S2D), consistent with the hypothesis that SCR maintains the stem cell niche and root growth by specifically suppressing *ARR1* expression.

SCR Directly Suppresses *ARR1* in the QC and Acts Non-Cell-Autonomously to Control ARR1 at the TZ

The fact that *SCR* is expressed exclusively in the QC and endodermal lineage implies that SCR regulates ARR1 cell-autonomously in the QC but that outside the QC its regulation is non-cell-autonomous.

To analyze SCR activity in the QC, we employed the GAL4VP16/UAS transactivation system (Brand and Perrimon, 1993; Sabatini et al., 2003). This allowed us to express an inducible version of the SCR protein fused to the glucocorticoid receptor (GR) in the *scr-4* mutant background and under control of the *WOX5* promoter and simultaneously mark the SCR:GR-expressing cells with GFP (*scr-4/pWOX5>>SCR:GR>>GFP* plants) (Figure S3A). Four hours of SCR:GR activation with dexamethasone (Dex) was sufficient to downregulate *ARR1* mRNA specifically in the QC region, as shown by qRT-PCR experiments on sorted QC cells (using fluorescence-activated cell sorting [FACS]) (Figure 3C). However, there was no change in expression in the rest of the root meristem, as visualized by *pARR1::ARR1:GUS* expression (Figures 3A and 3B, compare 0h Dex with 4h Dex). ARR1 downregulation was followed by recovery of stem cell activity, but not meristem size, after 8 hr of Dex treatment (Figures 3A, 3B, and 3D, compare 0h Dex with 8h Dex). This was coincident with the time when ARR1 expression was repositioned at the TZ (Figure 3A, 8h Dex). Root meristem size recovery occurred after 24 hr of Dex treatment (Figures 3A and 3D, 24h Dex). These results support the hypothesis that SCR suppresses *ARR1* expression in the QC to maintain stem cell activity. Importantly, these results also provide evidence that SCR acts on ARR1 non-cell-autonomously to position it at the TZ, thereby controlling meristem size.

To determine if SCR binds directly to the *ARR1* promoter, we performed chromatin immunoprecipitation (ChIP) followed by quantitative PCR (qPCR) on plants containing a complementing *SCR:GFP* chimeric protein under the control of its own promoter in the *scr-4* background. Initially, we used whole root meristems

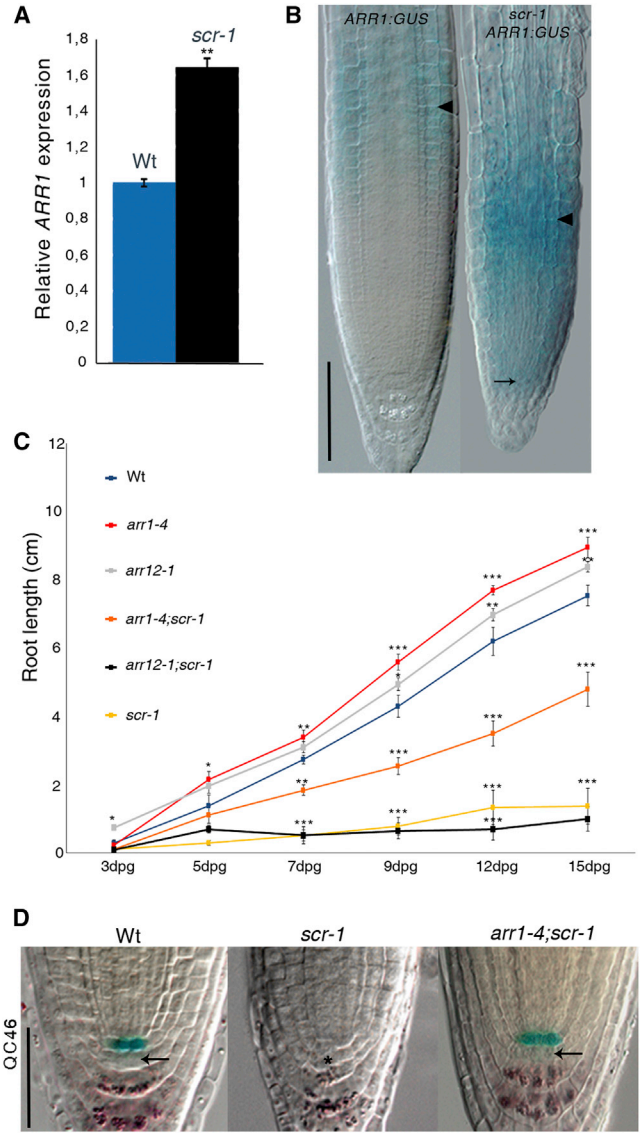

Figure 2. SCR Maintains SCN Activity by Suppressing ARR1

(A) qRT-PCR showing a low level of *ARR1* transcript in WT compared to *scr-1* roots. Relative expression is normalized to *ACTIN2*. Error bars represent SD; **p < 0.01 (Student's t test).

(B) Expression of *pARR1::ARR1:GUS* construct in WT roots and in *scr-1* mutant. Black arrowheads indicate the position of transition zone; arrow indicates ARR1 ectopic expression in the *scr-1* QC. Scale bar represents 100 μm.

(C) Root length measured over time for WT, *scr-1*, *arr1-4*, *arr12-1*, *arr1-4;scr-1*, and *arr12-1;scr-1*. Dpg, days postgermination. Error bars represent SD; *p < 0.05, **p < 0.01, ***p < 0.001 (Student's t test).

(D) *QC46* expression in, from left to right, WT, *scr-1*, and *arr1-4;scr-1*. Shown is double labeling of QC and differentiated columella cells visualized by QC46 and amyloplast staining, respectively. Note that black arrows indicate restoration of columella stem cells activity in the *arr1-4;scr-1* double mutant. Asterisk indicates the position of QC cells in the *scr-1* mutant. The same results have been obtained with the *arr1-3;scr-1*, *arr1-3;scr-4*, and *arr1- 4;scr-4* double-mutant combinations (data not shown). Scale bar represents 50 μm. See also Figure S2.

but found no enrichment for binding to the *ARR1* promoter region with the exception of region #3, where enrichment was not statistically significant (Figure S3B). If SCR binds the *ARR1* promoter specifically in the QC, we reasoned that we may have been diluting the ChIP signal when we used the entire meristem. Therefore, we next performed ChIP on extracts from dissected longitudinal sections (three to five cell lengths) that encompassed the QC (Brady et al., 2007). In this QC-enriched material, we found that binding to region #3 in the *ARR1* promoter was significantly enriched (Figure 3E), providing evidence that SCR directly binds to the *ARR1* promoter in the QC.

Suppression of *ARR1* Expression in the QC Titrates Auxin Production

We have previously shown that ARR1 promotes cell differentiation in the TZ by directly activating the *SHY2* gene (Dello Ioio et al., 2008). Therefore, we hypothesized that in the QC of *scr-1* roots, *SHY2* is activated by ARR1, which triggers the onset of differentiation. However, we did not detect ectopic expression of *SHY2* in the *scr-1* QC (data not shown), and elimination of *SHY2* activity in the *scr-1* mutant did not restore root growth and meristem size (Figures S2C and S2D). This suggests that ectopic expression of *ARR1* in the *scr* QC induces stem cell differentiation via a different mechanism.

It was recently shown that cytokinin can induce auxin biosynthesis in the *Arabidopsis* root apex (Jones et al., 2010) and that high levels of auxin in the SCN result in stem cell differentiation (Ding and Friml, 2010). We observed abnormally high levels of auxin in *scr-1* root meristems, as visualized by *DR5::GFP* expression (Sabatini et al., 1999; Ottenschläger et al., 2003) and as measured by mass spectrometry (Figures 4A and 4B). *DR5::GFP* localization reverted to normal in the *arr1-4;scr-1* double mutant (Figure 4A), suggesting that excess auxin biosynthesis in *scr-1* is induced by ectopic expression of *ARR1* in the QC. Among the auxin biosynthesis genes induced by cytokinin (Jones et al., 2010) and expressed in the QC (Sun et al., 2009; Bartel and Fink, 1994; http://bar.utoronto.ca/efp/cgi-bin/efpWeb.cgi), *NITRILASE 3* (*NIT3*), *NITRILASE 4* (*NIT4*), and *YUCCA6* (*YUC6*) are overexpressed in the *scr-1* mutant and revert to wild-type levels in the *arr1-4;scr-1* (Figure S4A). Since these genes control different branches of the tryptophan-dependent auxin biosynthesis pathway (Stepanova et al., 2011), we decided to prevent enzymatic redundant activities by focusing on the *ANTHRANILATE SYNTHASE BETA SUBUNIT 1* (*ASB1*) gene, which is expressed in the SCN and catalyzes a rate-limiting step of tryptophan biosynthesis (Stepanova et al., 2005). *ASB1* is induced by cytokinin, as visualized by the *pASB1::GUS* transcriptional fusion and confirmed by qRT-PCR (Figures S4B and S4C). Moreover, its induction is dependent on ARR1 function, since cytokinin treatment of the *arr1-4* mutant had no effect on *ASB1* levels (Figures S4B and S4C). In addition, a very brief staining of this transcriptional fusion shows that the expression of *ASB1* is highly upregulated in the QC of the *scr-1* mutant and reverted to wild-type levels in the *arr1-4;scr-1* double mutant (Figures 4C and S4D). This suggests that overexpression of *ASB1* in the *scr-1* mutant background depends on ARR1. To exclude the possibility that *ASB1* transcriptional activation is under the direct controls of SCR, we performed ChIP-qPCR analysis as described above for *ARR1*. Our ChIP-qPCR results

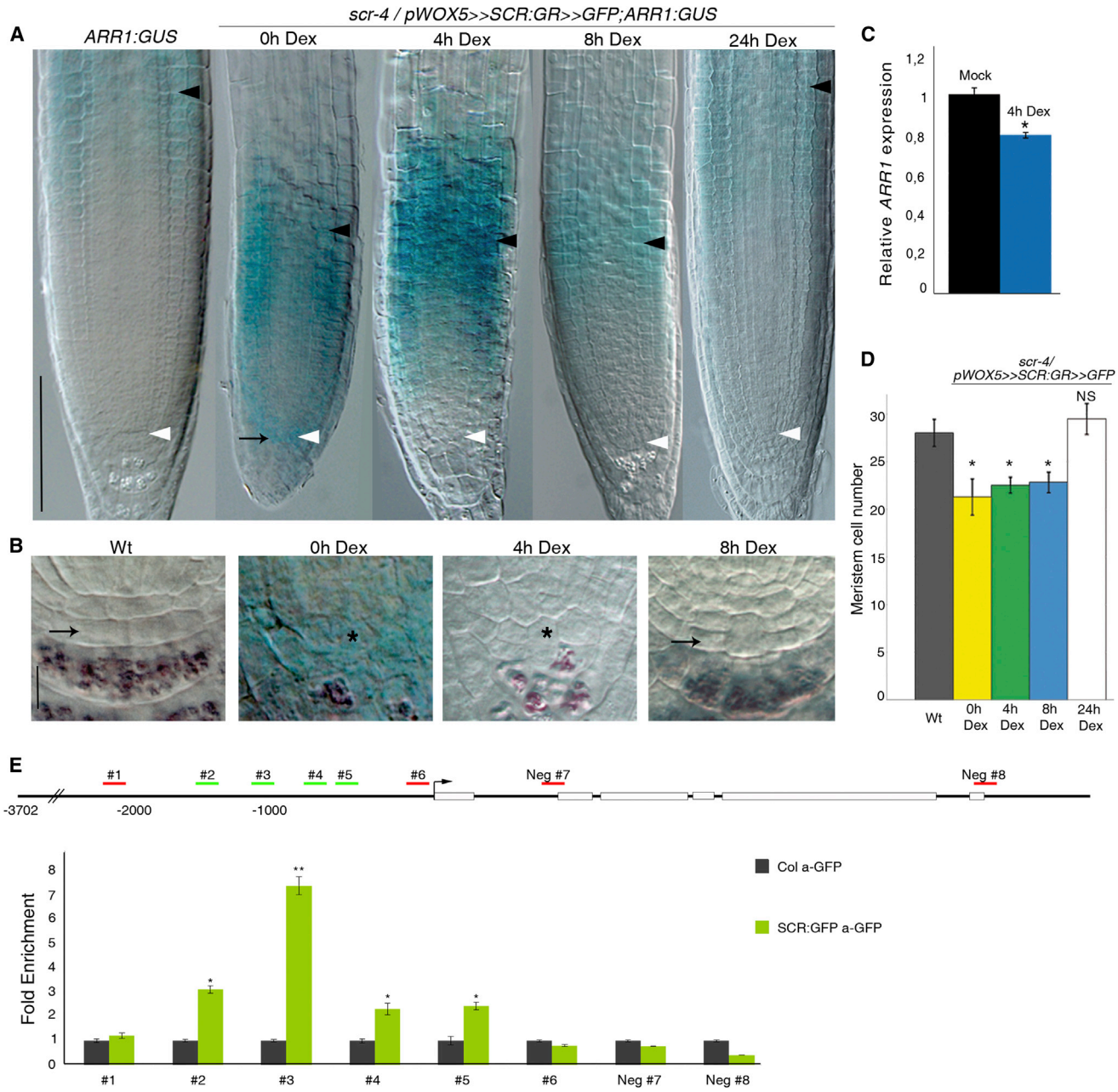

Figure 3. SCR Controls Stem Cell Activity by Directly Suppressing ARR1 in the QC

(A) Expression analysis of the *ARR1:GUS* translational fusion in, from left to right, WT and *scr-4/pWOX5>>SCR:GR>>GFP* roots untreated (0h Dex) or treated with Dex for 4, 8, and 24 hr. Black arrow indicates ectopic ARR1 expression in the QC. Black and white arrowheads indicate, respectively, the cortex TZ and the QC. Scale bar represents 100 μm.

(B) Stem cell niche of, from left to right, *ARR1:GUS* and *scr-4/ pWOX5>>SCR:GR>>GFP;ARR1:GUS* untreated (0h Dex) or treated with Dex for 4 and 8 hr. The black arrow indicates active stem cells in WT and *scr-4* roots after 8 hr of Dex treatment. Asterisk indicates the presumptive position of QC cells in *scr-4* untreated roots and in those treated with Dex for 4 hr. Scale bar represents 10 μm.

(C) qRT-PCR performed on sorted QC cells of *scr-4* roots carrying the *pWOX5>>SCR:GR>>GFP* construct, showing significant downregulation of *ARR1* transcription upon 4 hr of Dex treatment. Relative expression is normalized to *ACTIN2*. Error bars represent SD. *$p < 0.05$ (Student's t test).

(D) Meristem cell number of, from left to right, WT and *scr-4/pWOX5>>SCR:GR>>GFP* roots untreated (0h Dex) or treated with Dex for 4, 8, and 24 hr. Error bars represent SD. *$p < 0.05$; NS, not significant (Student's t test).

(E) ChIP-RT qPCR of the *ARR1* promoter using 5-day-old Col-0 (gray bars) and *pSCR::SCR:GFP scr-4* (green bars) plants. ChIP samples were prepared from QC-enriched material. qRT-PCR results are shown as fold enrichment compared to Col-0. We found significant enrichment for the several fragments (#2, #3, #4, and #5) bound by SCR by scanning the 2,186 kb of sequence upstream of *ARR1*. The data shown are representative of three independent biological experiments with similar results. Error bars show the SD of the ChIP-qPCR reactions performed in triplicate. *$p < 0.05$, **$p < 0.01$ (Student's t test).

See also Figure S3.

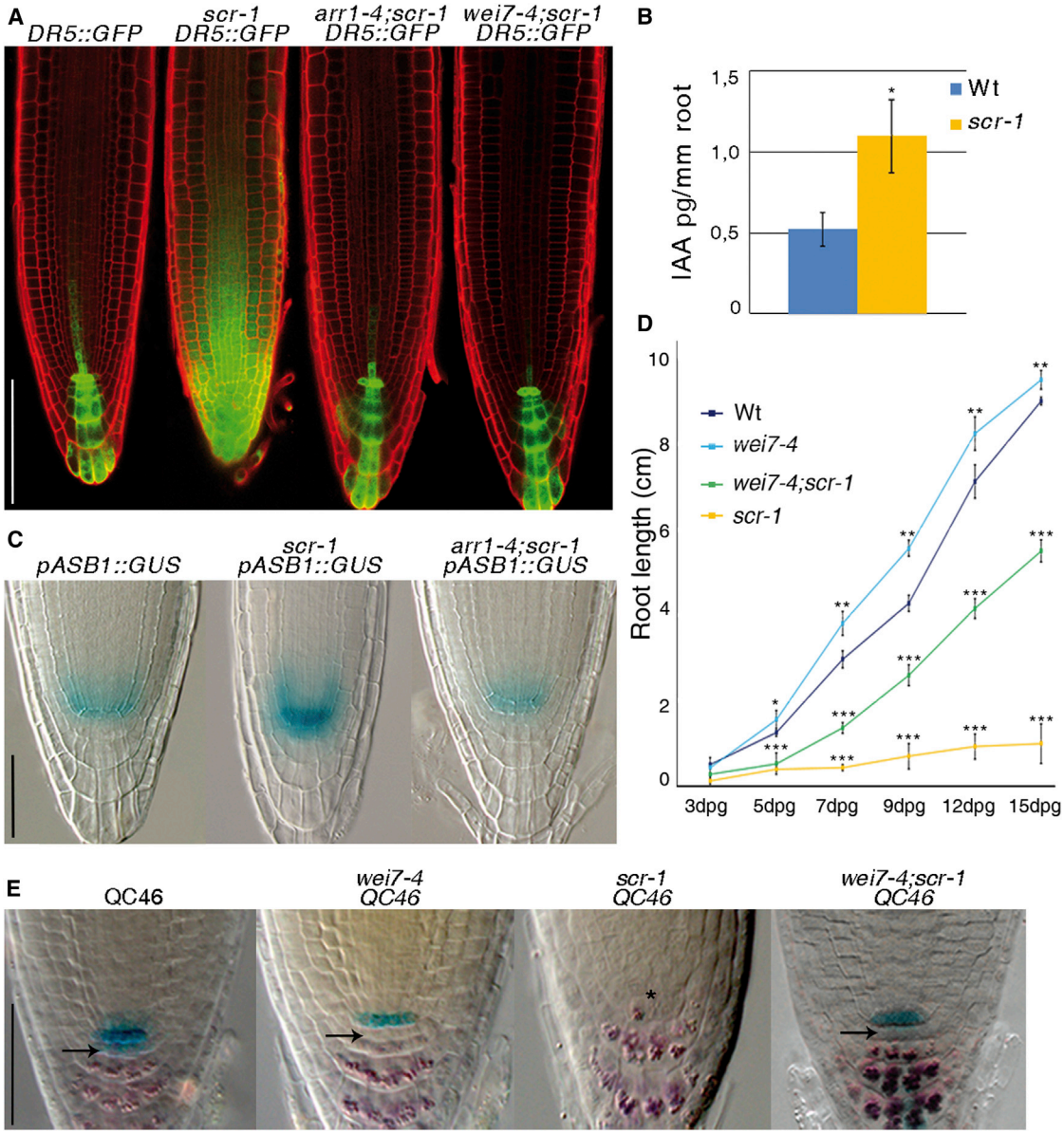

Figure 4. *SCR* Controls Auxin Biosynthesis in the QC via *ARR1*

(A) *DR5::GFP* expression in, from left to right, WT, *scr-1, arr1-4;scr-1*, and *wei7-4;scr-1* 5-day-old root meristems. Scale bar represents 100 μm.

(B) Concentration of free IAA in root tips of WT and *scr-1*. Error bars represent SD. *p < 0.05 (Student's t test).

(C) Expression of the *pASB1::GUS* construct in, from left to right, WT, *scr-1* and *arr1-4;scr-1*. Note that plants were stained for only 30 min. Scale bar represents 50 μm.

(D) Root length measured over time of WT, *scr-1*, *wei7-4*, and *wei7-4;scr-1*. Dpg, days postgermination. Error bars represent SD. *p < 0.05, **p < 0.01, ***p < 0.001 (Student's t test).

(E) *QC46* expression and Lugol staining of WT, *wei7-4*, *scr-1*, and *wei7-4;scr-1*. Black arrows indicate stem cells activity in WT, *wei7-4*, and *wei7-4;scr-1*. Asterisk indicates the presumptive position of QC cells in *scr-1*. The same result has been obtained with the *wei7-1;scr-1* double mutant combination. Scale bar represents 50 μm.

See also Figure S4.

suggest that SCR does not directly regulate *ASB1* (Figure S3C). Thus, in the QC of *scr-1*, loss of repression of *ARR1* leads to overexpression of *ASB1* and, consequently, overaccumulation of auxin in the root meristem.

To determine if overaccumulation of auxin is responsible for stem cell differentiation in *scr-1*, we introduced the ASB1 loss-of-function mutation *wei7-4* (*WEAK ETHYLENE INSENSITIVE 7*) (Stepanova et al., 2005) into the *scr-1* background. Consistent with our hypothesis, the root of *wei7-4;scr-1* displays a stable root meristem and indeterminate growth (Figures 4D and S4E) due to a functional SCN (Figures 4E and S4F). This phenotype is similar to the one of *arr1-4;scr-1* previously described (Figures

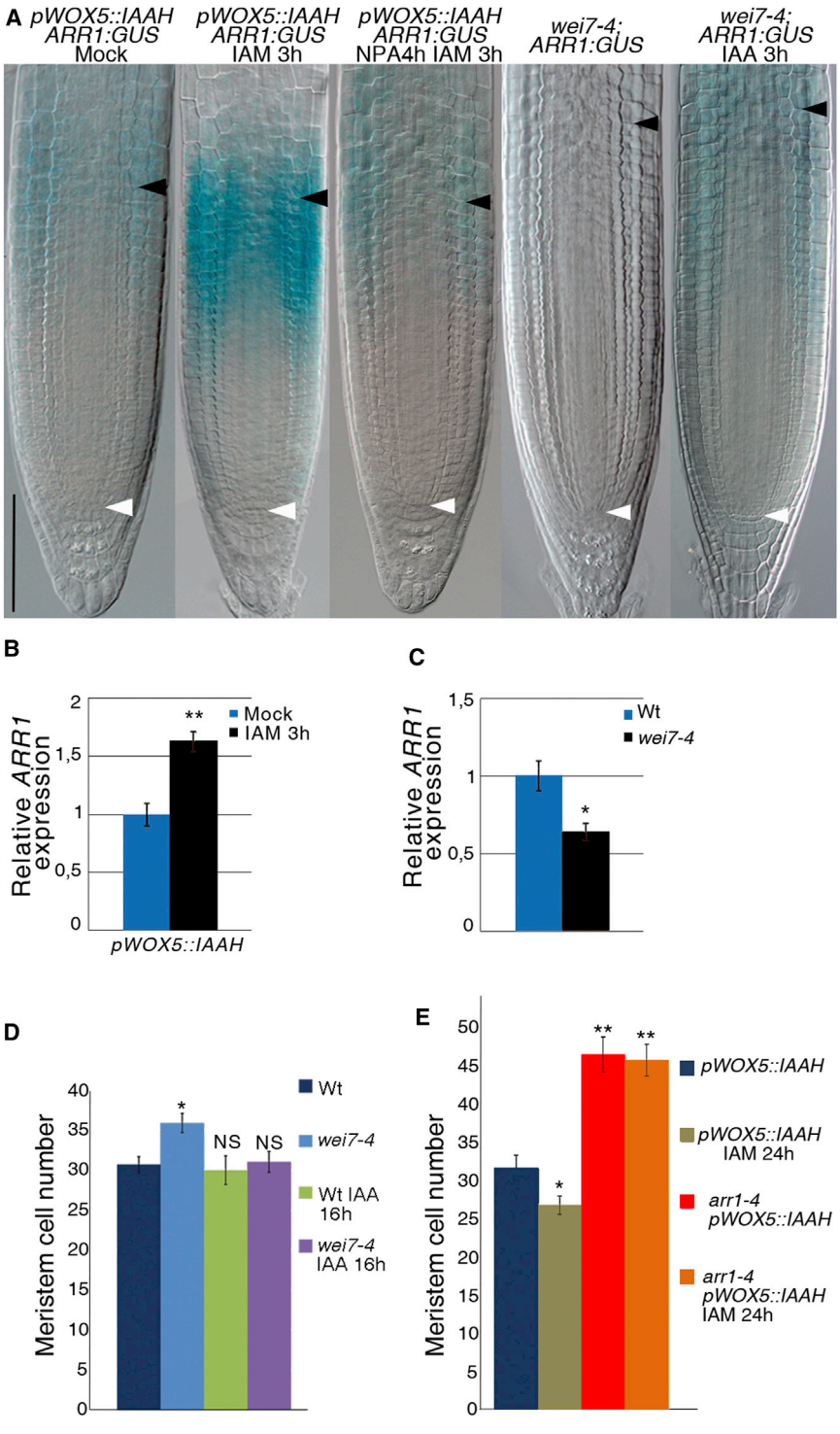

Figure 5. SCR Controls ARR1 Activity at the TZ via Auxin

(A) Expression of the *ARR1:GUS* translational fusion in, from left to right, mock-treated *pWOX5::IAAH* root, *pWOX5::IAAH* root treated with IAM, *pWOX5::IAAH* root treated with IAM and NPA, and *wei7-4* roots untreated or treated with IAA. Black and white arrowheads indicate, respectively, the cortex TZ and the QC. Roots were analyzed 5 dpg. Scale bar represents 100 μm.

(B) qRT-PCR showing upregulation of *ARR1* transcription in *pWOX5::IAAH* roots upon 3 hr of IAM treatment. Error bars represent SD. **p < 0.01 (Student's t test).

(C) qRT-PCR showing low *ARR1* transcript levels in *wei7-4*. Error bars represent SD. *p < 0.05 (Student's t test).

(D) Root meristem cell number in, from left to right, WT, *wei7-4,* WT upon 16 hr of IAA treatment, and *wei7-4* upon 16 hr of IAA treatment. Error bars represent SD. *p < 0.05; NS, not significant (Student's t test). Roots were analyzed 5 dpg.

(E) Root meristem cell number in, from left to right, mock-treated *pWOX5::IAAH* root, *pWOX5::IAAH* treated 24 hr with IAM, mock-treated *arr1-4;pWOX5::IAAH*, and *arr1-4;pWOX5::IAAH* treated for 24 hr with IAM. Error bars represent SD. *p < 0.05, **p < 0.01 (Student's t test). Roots were analyzed 5 dpg.

See also Figure S5.

2C and S2D). In addition, *DR5::GFP* expression in the root tip of *wei7-4;scr-1* reverted to lower levels compared to *scr-1* (Figure 4A), further supporting the hypothesis that *ASB1* upregulation in the *scr-1* QC is responsible for the abnormal accumulation of auxin in this mutant.

Therefore, our working model is that in *scr-1*, lack of *ARR1* repression in the QC cells leads to ASB1-dependent auxin over-accumulation responsible for stem cell inactivation, meristem consumption, and determinate root growth (Figure S4G). At the same time, we are showing that *SCR* can be induced by auxin (Figure S5A), thus generating a local feedback loop involved in homeostasis of auxin levels responsible for SCN activity.

SCR Regulates ARR1 Non-Cell-Autonomously through Auxin

We next asked if auxin could mediate the non-cell-autonomous effect of SCR on *ARR1* expression at the TZ (Figure 3A). We found that exogenous auxin application induces *ARR1* expression in the TZ (Figures S5B and S5C). To further test this hypothesis, we employed a construct expressing the *IAAH* gene, the bacterial auxin biosynthetic enzyme, driven by the *WOX5* promoter (*pWOX5::IAAH*) (Figure S5D) (Blilou et al., 2005). In *pWOX5::IAAH* plants, auxin biosynthesis can be induced specifically in the QC after indole-3-acetamide (IAM) auxin precursor treatment (Blilou et al., 2005). We observed that, as early as at 3 hr of IAM treatment, a QC-specific increase of auxin levels was sufficient to induce *ARR1* expression in the TZ but not in the QC (Figures 5A and 5B). To verify that auxin produced in the QC was transported in the TZ and that this resulted in *ARR1* transcriptional

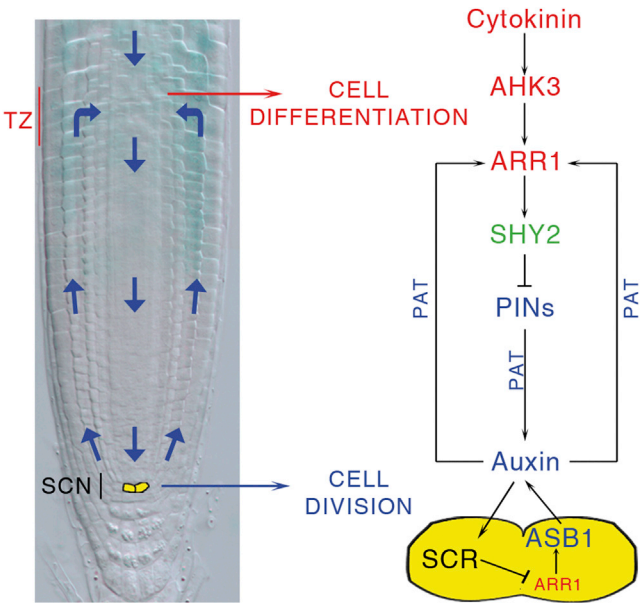

Figure 6. Model for the Spatial Coordination between SCN and TZ

Model showing how SCR presides over the spatial coordination between stem cell niche (SCN) and transition zone (TZ) activity. In the QC (yellow), SCR represses *ARR1*, which in turn controls auxin production via *ASB1*, thus enabling cell division along the transamplifying zone. SCR also exerts, via polar auxin transport (PAT), a long-distance control on *ARR1* at the TZ, enabling cytokinin to sustain cell differentiation via SHY2 (Dello Ioio et al., 2008).

activation, we treated plants in the presence of N-naphthylphthalamic acid (NPA), an inhibitor of auxin transport (Jacobs and Rubery, 1988). Production of auxin in the QC, via the *pWOX5*::*IAAH*/*IAM* system, resulted in accumulation of the auxin sensor *DR5::GFP* at the TZ. We could show that this accumulation is prevented via NPA treatment (Blilou et al., 2005) (Figure S5D). Interestingly, lack of *DR5::GFP* accumulation at the TZ upon NPA treatment was accompanied by lack of ARR1 induction at the TZ (Figure 5A), strongly suggesting that auxin is the non-cell-autonomous factor that controls ARR1 activity in the TZ from the QC.

To determine if ASB1-dependent auxin production in the QC could control ARR1 activity in the TZ, we analyzed *ARR1* expression in the *wei7-4* mutant. We observed lower *ARR1* mRNA and protein levels and an enlarged root meristem (Figures 5A, 5C, and 5D). Interestingly, ARR1 protein levels reverted to wild-type after 3 hr of exogenous auxin application (Figure 5A), followed by root meristem size complementation after 16 hr of auxin application (Figure 5D). We then asked if auxin produced in the QC is sufficient to induce cell differentiation in the TZ, and if so, if it acts through ARR1. Consistent with this hypothesis, we observed that the root meristem size of wild-type plants carrying a *pWOX5::IAAH* construct was reduced after 24 hr of IAM supplying, and thus of auxin production, while no meristem size reduction was observed when the same construct was introduced into the *arr1-4* background (Figure 5E). Taken together, these results indicate that auxin is the non-cell-autonomous signal, which originates in the QC and controls ARR1 activity in the TZ (Figure 6). We hypothesize that heightened levels of auxin induce cell differentiation in the TZ via the cytokinin-signaling pathway.

DISCUSSION

In both plants and animals, organ morphogenesis depends on the coordination between the activities of cells belonging to different tissues and at different developmental stages. In particular, SCN activity and differentiation of their progeny must be coordinated to ensure coherent growth. As observed in animal organogenesis (e.g., growth of mammalian bones or the gut crypt) (Spradling et al., 2001; Wolpert and Tickle, 2011), stem cell division and terminal differentiation of the progeny in the plant root take place in physically distinct zones separated by a group of transit-amplifying cells (Scheres, 2007; Sablowski, 2011). Here, we show that in *Arabidopsis*, the *SCR* gene acts from the QC to coordinate stem cell division and cell differentiation (model in Figure 6). It had been previously shown that SCR is necessary and sufficient to maintain the SCN (Sabatini et al., 2003) but the molecular mechanisms through which it sustains QC and stem cell activity are unknown. We show that SCR directly represses *ARR1* specifically in the QC, thereby repressing cytokinin-dependent cell differentiation and sustaining SCN activity (model in Figure 6). This is in line with what is already observed in animal systems, where master regulatory transcription factors mediate stem cell maintenance through direct transcriptional repression of factors that in turn would promote differentiation (Bernstein et al., 2006; Mikkelsen et al., 2007).

Ectopic expression of *ARR1* in the *scr-1* QC induces stem cell differentiation via a mechanism different from the one acting in the TZ, which relies on the transcriptional activation of the *SHY2* gene (Dello Ioio et al., 2008). In the QC, ARR1 regulates auxin production by modulating expression of the auxin biosynthesis gene *ASB1*. ASB1 controls a rate-limiting step in auxin biosynthesis and is specifically expressed in the SCN, being most active in the QC. Interestingly, other genes involved in auxin biosynthesis and acting downstream of the ASB1 pathway, such as TRYPTOPHAN AMINOTRANSFERASE OF *ARABIDOPSIS* 1 (TAA1) (Stepanova et al., 2008), NIT3 (Sun et al., 2009), CYTOCHROME P450 FAMILY 79 SUBFAMILY B POLYPEPTIDE 2 (CYP79B2), and CYP79B3 (Ljung et al., 2005) and YUCCA2 (YUC2) (Sun et al., 2009), are specifically expressed in the QC, thus suggesting that the QC is the primary source of auxin in the root meristem. A future challenge will be to understand how auxin produced in the QC controls the activity of the surrounding stem cells. Recently, it has been shown that SCR in the cortex/endodermis stem cell is part of a complex specifically involved in ground tissue stem cell asymmetric division (Cruz-Ramírez et al., 2012). The activity of this complex depends on auxin levels (Cruz-Ramírez et al., 2012), leading to the intriguing hypothesis that SCR, by controlling auxin biosynthesis in the QC, controls division of the other stem cell types modulating the activities of similar complexes. On the other hand, it is well known that titration of auxin levels in the SCN is critical to the maintenance of stem cell activity, since it has been shown that high levels of auxin promote stem cell differentiation (Ding and Friml, 2010).

By controlling the level of auxin production in the QC, SCR also exerts a long-distance control on *ARR1* in the TZ. Auxin produced by ASB1 in the QC, distributed in the meristem via the auxin transport facilitators (e.g., *PIN, PGP* genes) (Friml, 2010), is sufficient to activate expression of *ARR1* in the TZ, where ARR1 controls *SHY2* expression. SHY2 negatively controls

PIN's activities and auxin transport, enabling cytokinin to trigger differentiation of transit-amplifying cells (model in Figure 6) (Dello Ioio et al., 2008). It is worth mentioning that SCR, by controlling activity of the PHABULOSA gene (Carlsbecker et al., 2010) also controls ARR1 protein activity by regulating cytokinin biosynthesis in the vascular tissues (Dello Ioio et al., 2012).

In conclusion, we propose a model in which the SCN organizer not only controls division of the surrounding stem cells (van den Berg et al., 1997) but also regulates the differentiation of the transit-amplifying cells in the TZ. QC activity depends on SCR (Sabatini et al., 2003), which suppresses *ARR1*, thus titrating auxin production via the *ASB1* gene. Auxin produced in the QC not only controls stem cell division activity by an as-yet-unknown mechanism but at the same time acts as a long-distance signal to fine-tune the level of *ARR1* transcription in the TZ, thus controlling the rate of differentiation. In this way, a single gene, *SCR*, regulates the spatial coordination between stem cell division and differentiation, ensuring coherent root growth.

EXPERIMENTAL PROCEDURES

Plant Materials

The *Arabidopsis thaliana* ecotypes Columbia (Col-0), Wassilewskija (Ws), and Landsberg *erecta* (Ler) were used. *ahk3-3*, *arr1-4*, *arr1-3*, *arr12-1*, *wei7-4*, and *wei7-1* mutants are in Col-0 background (Dello Ioio et al., 2007, 2008; Stepanova et al., 2005), *shy2-31* mutant is in Ler background (Dello Ioio et al., 2008), and *scr-1* and *scr-4* mutants are in Ws background (Fukaki et al., 1998; Sabatini et al., 2003). *pAHK3::AHK3:GUS*, *pARR12::ARR12:GUS*, *pARR1::ARR1:GUS*, *pWOX5::GFP*, *QC25*, *QC46*, *DR5::GFP*, *pSCR::SCR:GFP*, *pWOX5:IAAH/DR5::GFP* and *pASB1::GUS* transgenic plants have been described previously (Dello Ioio et al., 2007, 2008; Blilou et al., 2005; Sabatini et al., 2003; Stepanova et al., 2005; Ottenschläger et al., 2003). The *Q1630* and *J0571* lines belong to the Haseloff collection (http://arabidopsis.info/CollectionInfo?id=24).

Plant Growth Conditions

Seeds were surface sterilized using 50% bleach for 10 minutes and then rinsed four times with sterile water. After 5 days of cold treatment, *A. thaliana* seeds were plated and grown, in a near-vertical position, at 22°C in long-day conditions (16 hr light/8 hr dark cycle) on one-half MS (Murashige and Skoog medium, Duchefa) supplemented with sucrose as previously described (Perilli and Sabatini, 2010). Plants for IAA measurement were grown as previously described (Ljung et al., 2005).

Root Length and Meristem Size Analysis

For root length measurements, plates were photographed and the resulting images were analyzed using the ImageJ software available online (http://rsbweb.nih.gov/ij/). For meristem size analysis, roots were prepared in a glass slide with chloralhydrate, as described in Perilli and Sabatini (2010), and then observed using an Axio Imager.A2 (Zeiss) light microscopy. To measure root meristem size, the number of cortical cells along a cell file (from the QC to the first elongated cell) were counted. To measure root development over time, root length and meristem size were analyzed at different days postgermination (dpg): 3 dpg, 5 dpg, 7 dpg, 9 dpg, 12 dpg, and 15 dpg. For each experiment, at least 90 roots were analyzed and the mean and SD were calculated.

Hormonal Treatments

The 5-day old seedlings were transferred to solid one-half MS medium containing mock conditions or a suitable concentration of hormone. For auxin treatment, we used indole-3-acetic acid (IAA, Duchefa) at a final concentration of 5 μM, prepared from a 10 mM stock in ethanol. Plants were treated for 2, 3, and 16 hr. For cytokinin treatment, we used *trans*-zeatin (tZ, Duchefa) at a final concentration of 5 μM, prepared from a 30 mM stock in 1N NaOH. Plants were treated for 4 hr. For auxin induction specifically within QC cells, plants carrying the *pWOX5::IAAH* construct, in wild-type and in *arr1-4* mutant background, were treated for 3 hr with 10 μM indole-3-acetamide (IAM, Sigma-Aldrich), a precursor of IAA, prepared from a 10 mM stock in DMSO. To inhibit auxin transport, plants were pretreated 1 hr with 50 μM NPA (Duchefa) and then treated for 3 hr with both 10 μM IAM and 50 μM NPA together. For each experiment, at least 90 roots were analyzed.

GUS Histochemical Assay

To visualize *QC25*, *QC46*, *pASB1::GUS*, *pAHK3::AHK3:GUS* *pARR12::ARR12:GUS* and *pARR1::ARR1:GUS* lines, GUS histochemical assay was performed using the β-glucuronidase substrate X-gluc (5-bromo-4-chloro-3-indolyl glucuronide, Duchefa) dissolved in N-N-dimethyl-formamide. X-gluc solution, composed of 100 mM Na_2HPO_4, 100 mM NaH_2PO_4, 0.5 mM K_3 $Fe(CN)_6$, 0.5 mM $K_4Fe(CN)_6$, 0.1% Triton X-100, and 1 mg/ml X-gluc, was prepared as previously described (Perilli and Sabatini, 2010). Five-day old seedlings were incubated for 16 hr at 37°C in the dark and imaged using the Axio Imager.A2 (Zeiss) microscopy. *pASB1::GUS* in Figure 4C was stained for 30 min only. For each experiment, at least 90 roots were analyzed.

Lugol Staining

Starch granules in the root tips were stained with Lugol solution (Carlo Erba Reagenti) for few seconds and then immediately observed and photographed at microscopy as previously described (van den Berg et al., 1997; Sabatini et al., 2003).

Confocal Image Processing

Confocal images of median longitudinal sections of 5-day-old roots were taken using a Zeiss LSM 780 microscope. A 10 μg/ml propidium iodide (Sigma) solution was used to visualize the cell wall.

Analysis of ARR1 Expression In Vivo using GUS Histochemical Assay

In vivo analysis of ARR1 expression in SCR:GR plants after Dex treatment were performed as follows: *scr-4/pWOX5>>SCR:GR>>GFP;pARR1::ARR1:GUS* were treated for 4, 8, and 24 hr with 2 μM Dex or an equivalent amount of DMSO as mock treatment. After Dex treatment, plants were stained 16 hr for the β-glucuronidase activity of *pARR1::ARR1:GUS* transgene and visualized as described above. Starch granules were visualized and meristem cell number was counted as described above (Dello Ioio et al., 2007; Sabatini et al., 2003; Perilli and Sabatini, 2010). To analyze the long-distance effect of both auxin and polar auxin transport on *ARR1*, 5-day-old *pWOX5::IAAH;pARR1::ARR1:GUS* plants were treated for 3 hr with 10 μM IAM and with both 10 μM IAM and 50 μM NPA as described above. After treatment, plants were stained for 16 hr for the β-glucuronidase activity of *pARR1::ARR1:GUS* transgene and visualized as described previously (Dello Ioio et al., 2007; Perilli and Sabatini, 2010). Meristem cell numbers were counted as described above. For exogenous auxin application, plants were treated for 3 hr with 5 μM IAA and stained as described above. For each experiment, at least 90 roots were analyzed.

FACS and qRT-PCR Experiments

scr-4/pWOX5>>SCR:GR>>GFP seeds were plated, on top of nylon mesh (Nitex 03-100/44, Sefar America), on one-half MS agar (+1% sucrose) plates at a density of approximately 500 seeds per row 5-day-old seedlings were transferred onto plates containing 10 μM Dex (Sigma-Aldrich), prepared from a 10 mM stock in DMSO, or an equivalent amount of DMSO, as mock treatment. Root tips (3–4 mm) were collected 4 hr after Dex treatment and protoplasted. QC cells expressing GFP were isolated on a fluorescence-activated cell sorter (Becton Dickinson FACSAriaII) as described elsewhere (Nawy et al., 2005). Sorted cells were collected directly into a RNA lysis buffer (QIAGEN RLT buffer, RNeasy Micro kit), mixed, and immediately frozen at −80°C. Experiments were carried out in two consecutive days, obtaining two biological replicates for each treatment (mock and Dex). mRNA was later isolated and treated with DNase using TURBO DNA-free Kit. Each RNA sample was reverse transcribed using the SuperScript III first-strand Synthesis system (Invitrogen) according to the manufacturer's instructions. qRT-PCR was performed in triplicates from each RNA sample and repeated twice using SYBR Green PCR Master mix (Applied Biosystems) with the ViiA 7 real-time PCR system (Applied Biosystems). Expression levels were calculated relative to *ACTIN2* using the $2^{-\Delta\Delta ct}$ method. Statistical analysis was done in MS Excel (ANOVA: single factor) using $p < 0.05$. Primers were designed according to

the recommendations of Applied Biosystems. qRT-PCR analysis was conducted using following gene-specific primers:

ARR1 FW: 5′-TTGAAGAAACCGCGTGTCGTCT-3′ and ARR1 RV: 5′-CCTTCTCAACGCCGAGCTGATTAA-3′ for *ARR1*
ACT FW: 5′-CCTTCTCAACGCCGAGCTGATTAA-3′ and ACT RV: 5′-GTGGATTCCAGCAGCTTCCAT-3′ for *ACTIN2*

ChIP followed by Gene-Specific qRT-PCR

ChIP was conducted as described in Sozzani et al. (2010) on either Col-0, as control, or *pSCR::SCR:GFP/scr-4* 5-day-old dissected roots, which included longitudinal sections composed of three to five cell lengths from the QC as described in Brady et al. (2007). Immunoprecipitation was done using a rabbit polyclonal antibody to GFP (ab290; Abcam). DNA from the ChIP, for both Col-0 and pSCR::SCR:GFP experiments, was individually amplified using a random-primer-based genome amplification method according to the Agilent Mammalian ChIP-on-chip protocol with minor modifications. Briefly, chromatin from the Col-0 and pSCR::SCR:GFP was blunted using T4 DNA polymerase, then linkers were added using T4 DNA ligase (oligo JW102 5′-GCG GTGACCCGGGAGATCTGAATTC-3′ and oligo JW103 5′-GAATTCAGATC-3′). The immunoprecipitate was then amplified with 15 PCR cycles (first LM-PCR) and then the reaction was diluted and used as template for a second round of 20 cycles (second LM-PCR). The DNA was cleaned up each time using the MiniElute Reaction Cleanup kit (QIAGEN). Enrichment of the ARR1 putative target promoter-region DNA was determined using qRT-PCR. A qPCR efficiency of 2-fold amplifications per cycle was assumed, and sequences from ubiquitin 10 (UBQ10) were used to normalize the results between samples (see Supplemental Experimental Procedures for primer sequences). Tiling along the *At3G16857 ARR1* gene was done using specific primers along the putative 2,186 kb region of the *ARR1* promoter (see Supplemental Experimental Procedures for primer sequences).

Tiling along the *AT1G25220 ASB1* gene was done using specific primers along the putative *ASB1* promoter (see Supplemental Experimental Procedures for primer sequences). Detailed descriptions of the transgenic lines construction and analysis, ChIP techniques, and transcript-level analysis are provided in the Supplemental Experimental Procedures.

IAA Quantification

Root tips (3 mm) from 20 4-day-old seedlings were collected and pooled for IAA quantification. A total of 150 pg $^{13}C_6$-IAA was added as internal standard to each sample before purification and analysis by gas chromatography selected-reaction-monitoring mass spectrometry as described previously (Edlund et al., 1995).

SUPPLEMENTAL INFORMATION

Supplemental Information includes Supplemental Experimental Procedures and five figures and can be found with this article online at http://dx.doi.org/10.1016/j.devcel.2013.06.025.

ACKNOWLEDGMENTS

We thank Ben Scheres and Marta Del Bianco for reading the manuscript, José M. Alonso for providing material, and Leonardo Giustini for technical support. This work was supported by grants from the European Research Council (to S.S., L.M., and S.P.), the Plant Stem Cell Network within the European Research Area in Plant Genomics framework (grant BB/E024858 to I.T.), the Giovanni Armenise-Harvard Foundation (to R.S.), the Centre for BioSystems Genomics of the Netherlands Genomics Initiative/Netherlands Organization for Scientific Research (to. D.B.), the Horizon program (to R.H.), the Istituto Pasteur-Fondazione Cenci Bolognetti, MIUR PRIN, and MIUR FIRB ERA-PG (to P.C.).

Received: August 10, 2012
Revised: May 20, 2013
Accepted: June 26, 2013
Published: August 26, 2013

REFERENCES

Bartel, B., and Fink, G.R. (1994). Differential regulation of an auxin-producing nitrilase gene family in Arabidopsis thaliana. Proc. Natl. Acad. Sci. USA *91*, 6649–6653.

Bernstein, B.E., Mikkelsen, T.S., Xie, X., Kamal, M., Huebert, D.J., Cuff, J., Fry, B., Meissner, A., Wernig, M., Plath, K., et al. (2006). A bivalent chromatin structure marks key developmental genes in embryonic stem cells. Cell *125*, 315–326.

Blilou, I., Xu, J., Wildwater, M., Willemsen, V., Paponov, I., Friml, J., Heidstra, R., Aida, M., Palme, K., and Scheres, B. (2005). The PIN auxin efflux facilitator network controls growth and patterning in Arabidopsis roots. Nature *433*, 39–44.

Brady, S.M., Orlando, D.A., Lee, J.Y., Wang, J.Y., Koch, J., Dinneny, J.R., Mace, D., Ohler, U., and Benfey, P.N. (2007). A high-resolution root spatiotemporal map reveals dominant expression patterns. Science *318*, 801–806.

Brand, A.H., and Perrimon, N. (1993). Targeted gene expression as a means of altering cell fates and generating dominant phenotypes. Development *118*, 401–415.

Carlsbecker, A., Lee, J.Y., Roberts, C.J., Dettmer, J., Lehesranta, S., Zhou, J., Lindgren, O., Moreno-Risueno, M.A., Vatén, A., Thitamadee, S., et al. (2010). Cell signalling by microRNA165/6 directs gene dose-dependent root cell fate. Nature *465*, 316–321.

Cruz-Ramírez, A., Díaz-Triviño, S., Blilou, I., Grieneisen, V.A., Sozzani, R., Zamioudis, C., Miskolczi, P., Nieuwland, J., Benjamins, R., Dhonukshe, P., et al. (2012). A bistable circuit involving SCARECROW-RETINOBLASTOMA integrates cues to inform asymmetric stem cell division. Cell *150*, 1002–1015.

Cui, H., Levesque, M.P., Vernoux, T., Jung, J.W., Paquette, A.J., Gallagher, K.L., Wang, J.Y., Blilou, I., Scheres, B., and Benfey, P.N. (2007). An evolutionarily conserved mechanism delimiting SHR movement defines a single layer of endodermis in plants. Science *316*, 421–425.

Dello Ioio, R., Linhares, F.S., Scacchi, E., Casamitjana-Martinez, E., Heidstra, R., Costantino, P., and Sabatini, S. (2007). Cytokinins determine Arabidopsis root-meristem size by controlling cell differentiation. Curr. Biol. *17*, 678–682.

Dello Ioio, R., Nakamura, K., Moubayidin, L., Perilli, S., Taniguchi, M., Morita, M.T., Aoyama, T., Costantino, P., and Sabatini, S. (2008). A genetic framework for the control of cell division and differentiation in the root meristem. Science *322*, 1380–1384.

Dello Ioio, R., Galinha, C., Fletcher, A.G., Grigg, S.P., Molnar, A., Willemsen, V., Scheres, B., Sabatini, S., Baulcombe, D., Maini, P.K., and Tsiantis, M. (2012). A PHABULOSA/cytokinin feedback loop controls root growth in Arabidopsis. Curr. Biol. *22*, 1699–1704.

Di Laurenzio, L., Wysocka-Diller, J., Malamy, J.E., Pysh, L., Helariutta, Y., Freshour, G., Hahn, M.G., Feldmann, K.A., and Benfey, P.N. (1996). The SCARECROW gene regulates an asymmetric cell division that is essential for generating the radial organization of the Arabidopsis root. Cell *86*, 423–433.

Ding, Z., and Friml, J. (2010). Auxin regulates distal stem cell differentiation in Arabidopsis roots. Proc. Natl. Acad. Sci. USA *107*, 12046–12051.

Edlund, A., Eklöf, S., Sundberg, B., Moritz, T., and Sandberg, G. (1995). A Microscale Technique for Gas Chromatography-Mass Spectrometry Measurements of Picogram Amounts of Indole-3-Acetic Acid in Plant Tissues. Plant Physiol. *108*, 1043–1047.

Friml, J. (2010). Subcellular trafficking of PIN auxin efflux carriers in auxin transport. Eur. J. Cell Biol. *89*, 231–235.

Fukaki, H., Wysocka-Diller, J., Kato, T., Fujisawa, H., Benfey, P.N., and Tasaka, M. (1998). Genetic evidence that the endodermis is essential for shoot gravitropism in Arabidopsis thaliana. Plant J. *14*, 425–430.

Heidstra, R., Welch, D., and Scheres, B. (2004). Mosaic analyses using marked activation and deletion clones dissect Arabidopsis SCARECROW action in asymmetric cell division. Genes Dev. *18*, 1964–1969.

Hwang, I., Sheen, J., and Müller, B. (2012). Cytokinin signaling networks. Annu. Rev. Plant Biol. *63*, 353–380.

Jacobs, M., and Rubery, P.H. (1988). Naturally occurring auxin transport regulators. Science *241*, 346–349.

Jones, B., Gunneråas, S.A., Petersson, S.V., Tarkowski, P., Graham, N., May, S., Dolezal, K., Sandberg, G., and Ljung, K. (2010). Cytokinin regulation of auxin synthesis in Arabidopsis involves a homeostatic feedback loop regulated via auxin and cytokinin signal transduction. Plant Cell *22*, 2956–2969.

Lee, M.H., Kim, B., Song, S.K., Heo, J.O., Yu, N.I., Lee, S.A., Kim, M., Kim, D.G., Sohn, S.O., Lim, C.E., et al. (2008). Large-scale analysis of the GRAS gene family in Arabidopsis thaliana. Plant Mol. Biol. *67*, 659–670.

Ljung, K., Hull, A.K., Celenza, J., Yamada, M., Estelle, M., Normanly, J., and Sandberg, G. (2005). Sites and regulation of auxin biosynthesis in Arabidopsis roots. Plant Cell *17*, 1090–1104.

Mikkelsen, T.S., Ku, M., Jaffe, D.B., Issac, B., Lieberman, E., Giannoukos, G., Alvarez, P., Brockman, W., Kim, T.K., Koche, R.P., et al. (2007). Genome-wide maps of chromatin state in pluripotent and lineage-committed cells. Nature *448*, 553–560.

Mondal, B.C., Mukherjee, T., Mandal, L., Evans, C.J., Sinenko, S.A., Martinez-Agosto, J.A., and Banerjee, U. (2011). Interaction between differentiating cell- and niche-derived signals in hematopoietic progenitor maintenance. Cell *147*, 1589–1600.

Moubayidin, L., Di Mambro, R., and Sabatini, S. (2009). Cytokinin-auxin crosstalk. Trends Plant Sci. *14*, 557–562.

Moubayidin, L., Perilli, S., Dello Ioio, R., Di Mambro, R., Costantino, P., and Sabatini, S. (2010). The rate of cell differentiation controls the Arabidopsis root meristem growth phase. Curr. Biol. *20*, 1138–1143.

Nawy, T., Lee, J.Y., Colinas, J., Wang, J.Y., Thongrod, S.C., Malamy, J.E., Birnbaum, K., and Benfey, P.N. (2005). Transcriptional profile of the Arabidopsis root quiescent center. Plant Cell *17*, 1908–1925.

Ottenschläger, I., Wolff, P., Wolverton, C., Bhalerao, R.P., Sandberg, G., Ishikawa, H., Evans, M., and Palme, K. (2003). Gravity-regulated differential auxin transport from columella to lateral root cap cells. Proc. Natl. Acad. Sci. USA *100*, 2987–2991.

Perilli, S., and Sabatini, S. (2010). Analysis of root meristem size development. Methods Mol. Biol. *655*, 177–187.

Perilli, S., Moubayidin, L., and Sabatini, S. (2010). The molecular basis of cytokinin function. Curr. Opin. Plant Biol. *13*, 21–26.

Pysh, L.D., Wysocka-Diller, J.W., Camilleri, C., Bouchez, D., and Benfey, P.N. (1999). The GRAS gene family in Arabidopsis: sequence characterization and basic expression analysis of the SCARECROW-LIKE genes. Plant J. *18*, 111–119.

Sabatini, S., Beis, D., Wolkenfelt, H., Murfett, J., Guilfoyle, T., Malamy, J., Benfey, P.N., Leyser, O., Bechtold, N., Weisbeek, P., and Scheres, B. (1999). An auxin-dependent distal organizer of pattern and polarity in the Arabidopsis root. Cell *99*, 463–472.

Sabatini, S., Heidstra, R., Wildwater, M., and Scheres, B. (2003). SCARECROW is involved in positioning the stem cell niche in the Arabidopsis root meristem. Genes Dev. *17*, 354–358.

Sablowski, R. (2011). Plant stem cell niches: from signalling to execution. Curr. Opin. Plant Biol. *14*, 4–9.

Sarkar, A.K., Luijten, M., Miyashima, S., Lenhard, M., Hashimoto, T., Nakajima, K., Scheres, B., Heidstra, R., and Laux, T. (2007). Conserved factors regulate signalling in Arabidopsis thaliana shoot and root stem cell organizers. Nature *446*, 811–814.

Scheres, B. (2007). Stem-cell niches: nursery rhymes across kingdoms. Nat. Rev. Mol. Cell Biol. *8*, 345–354.

Sozzani, R., Cui, H., Moreno-Risueno, M.A., Busch, W., Van Norman, J.M., Vernoux, T., Brady, S.M., Dewitte, W., Murray, J.A., and Benfey, P.N. (2010). Spatiotemporal regulation of cell-cycle genes by SHORTROOT links patterning and growth. Nature *466*, 128–132.

Spradling, A., Drummond-Barbosa, D., and Kai, T. (2001). Stem cells find their niche. Nature *414*, 98–104.

Stepanova, A.N., Hoyt, J.M., Hamilton, A.A., and Alonso, J.M. (2005). A Link between ethylene and auxin uncovered by the characterization of two root-specific ethylene-insensitive mutants in Arabidopsis. Plant Cell *17*, 2230–2242.

Stepanova, A.N., Robertson-Hoyt, J., Yun, J., Benavente, L.M., Xie, D.Y., Dolezal, K., Schlereth, A., Jürgens, G., and Alonso, J.M. (2008). TAA1-mediated auxin biosynthesis is essential for hormone crosstalk and plant development. Cell *133*, 177–191.

Stepanova, A.N., Yun, J., Robles, L.M., Novak, O., He, W., Guo, H., Ljung, K., and Alonso, J.M. (2011). The Arabidopsis YUCCA1 flavin monooxygenase functions in the indole-3-pyruvic acid branch of auxin biosynthesis. Plant Cell *23*, 3961–3973.

Sun, J., Xu, Y., Ye, S., Jiang, H., Chen, Q., Liu, F., Zhou, W., Chen, R., Li, X., Tietz, O., et al. (2009). Arabidopsis ASA1 is important for jasmonate-mediated regulation of auxin biosynthesis and transport during lateral root formation. Plant Cell *21*, 1495–1511.

Tian, Q., Uhlir, N.J., and Reed, J.W. (2002). Arabidopsis SHY2/IAA3 inhibits auxin-regulated gene expression. Plant Cell *14*, 301–319.

Tsukagoshi, H., Busch, W., and Benfey, P.N. (2010). Transcriptional regulation of ROS controls transition from proliferation to differentiation in the root. Cell *143*, 606–616.

van den Berg, C., Willemsen, V., Hendriks, G., Weisbeek, P., and Scheres, B. (1997). Short-range control of cell differentiation in the Arabidopsis root meristem. Nature *390*, 287–289.

Wolpert, L., and Tickle, C. (2011). Principles of Development (New York: Oxford University Press).

Wysocka-Diller, J.W., Helariutta, Y., Fukaki, H., Malamy, J.E., and Benfey, P.N. (2000). Molecular analysis of SCARECROW function reveals a radial patterning mechanism common to root and shoot. Development *127*, 595–603.